Optimization of Ti/Ta2O5–SnO2 electrodes and reaction parameters for electrocatalytic oxidation of methylene blue

Shestakova, M., Graves, J., Sitarz, M. & Sillanpää, M.

DOI 10.1007/s10800-016-0925-5
ISSN 0021-891X
ESSN 1572-8838
Publisher: Springer

Optimization of Ti/Ta_2O_5-SnO_2 electrodes and reaction parameters for electrocatalytic oxidation of methylene blue

Marina Shestakova[a], John Graves[b], Maciek Sitarz[c], Mika Sillanpää[a]*

[a] *Laboratory of Green Chemistry, Faculty of Technology, Lappeenranta University of Technology, Sammonkatu 12, FI-50130 Mikkeli, Finland*

[b] *Functional Materials Applied Research Group, Coventry University, Priory Street, Coventry, CV1 5FB, United Kingdom.*

[c] *AGH University of Science and Technology, Faculty of Materials Science and Ceramics, Av. Mickiewicza 30, 30-059 Cracow, Poland*.

*Corresponding author. Tel.: +358 50 594 8015. E-mail address: marina.shestakova@hotmail.com (M. Shestakova).

Abstract

Among existing water treatment methods for organic containing wastewaters advanced oxidation processes (AOP) and particularly electrocatalytic oxidation is a technique allowing to reach high degradation and mineralization efficiencies. Electrodes tested for use in electrocatalytic oxidation processes contain either expensive or platinum/group metals such as Pt, Ru, Ir, Pd or boron doped diamond (BDD) and Sb and Pb compounds which are toxic for the environment. Thereby, there is a need for environmentally friendly and less expensive electrodes. The objectives of this research were to optimize annealing temperature of Ti/Ta_2O_5-SnO_2 electrodes, establish the working media for organic compound oxidation processes as well as check degradation, mineralization and current efficiencies for methylene blue (MB) dye oxidation. Decolourisation efficiency of 95% was achieved in 2h at pH = 6.5. Neutral media showed also higher efficiency towards COD decrease which was equal to 85% after 2 h of electrolysis. The lowest energy consumption of 7.7 kWh m^{-3} required for 100% decolourisation was observed for the electrodes annealed at 550 ^{0}C at pH = 2. The highest current efficiency (CE) of 10.1% attributed to 80% of COD reduction was obtained for the electrode annealed at 550 ^{0}C at pH = 6.5. The optimization data allow further extrapolating of electrocatalytic oxidation process on Ti/Ta_2O_5-SnO_2 electrodes to pilot scale.

Keywords. Electrocatalysis, Electrolysis, Ti/Ta_2O_5-SnO_2 electrodes, Methylene Blue

1 Introduction

Water, energy, food and climate securities are the main global challenges nowadays where water is the core of the water-food-energy-climate nexus [1]. Spent industrial and domestic water cannot be directly released back to the environment or returned to a technological cycle since it is contaminated with mechanical impurities, organic and inorganic pollutants.

Traditional treatment methods of wastewater containing organic compounds are biological treatment, chemical oxidation, coagulation and adsorption. However, these methods are inefficient towards persistent organic compounds such as insecticides, pesticides, pharmaceuticals etc. [2] In addition, a significant group of pollutants such as dyes which are widely used in textile, tannery, pulp and paper and pharmaceutical industries were found resistant to microorganism attack and cannot be efficiently treated by biological methods [3]. Despite the ease of implementation, all traditional wastewater treatment methods have the main disadvantage of the secondary waste formation. Spent adsorbents, coagulation, sedimentation and sewage sludge should be regenerated or disposed which requires additional costs and working areas.

Advanced oxidation processes (AOP) and particularly electrocatalytic oxidation are promising techniques allowing a complete mineralization of resistant organic pollutants to simple molecules like CO_2 and H_2O without generation of secondary wastes. Electrocatalytic oxidation of organic pollutants by direct electrolysis occurs by means of interaction of adsorbed hydroxyl radicals on the electrode surface (M) with an organic pollutant (R) [4-5]:

$$M(H_2O) \rightarrow M(^{\cdot}OH) + H^+ + e^- \quad (1)$$

$$R + M(^{\cdot}OH)_n \rightarrow M + \text{Oxidation products} + nH^+ + ne^- \quad (2)$$

Moreover, along with high mineralization efficiencies achieved by anodic oxidation, electrocatalytic methods are easy to implement and automate. The most commonly used electrodes for electrocatalytic oxidation of organic compounds are BDD, Pt, Sb-doped RuO_2/TiO_2, Ti/IrO_2-SnO_2-Sb_2O_5, Ti–Pt/β-PbO_2, Ti/Sb-SnO_2, Ti/PbO_2, Ti/(IrO_2+Ta_2O_5), Ti/SnO_2–Sb_2O_5, Ti/SnO_2–Sb_2O_5–PtO_x, Ti/SnO_2–Sb_2O_5–RuO_2, Ti/RuO_2-IrO_2 [6-15]. As it can be seen all of them contain either expensive compounds like diamond, Pt, Ru, Ir or potentially environmentally toxic compounds such as Pb and Sb. Therefore there is a search for less expensive, less toxic electrodes with a high electrocatalytic oxidation efficiency. Over the last few years phosphotungstic acid/neutral red intercalated montmorillonite composite (PTA/NR–MMT) film electrodes assembled on a graphite electrode, magnetite/reduced graphene oxide (Fe_3O_4/RGO) composite electrodes, Ni-doped nanoporous carbon electrodes, lithium-doped Ta_2O_5

film coated electrodes etc. were found active towards oxidation of N-acetylcysteine, methyl jasmonate, propargyl alcohol, ascorbic acid and glucose [16-20]. However, the above mentioned electrodes have been only electrochemically and physically characterized and so far, there is no information on electrolysis experiments, degradation efficiencies, COD and TOC decrease of organic pollutants using these types of electrodes. Moreover, carbon-containing electrodes are expected to be suitable for detection of organic compounds rather than for their oxidation in wastewaters due to low potential for carbon corrosion [21] which is shown in the following reactions:

$C + 2H_2O \rightarrow CO_2 + 4H^+ + 4e^-$, $E^0 = 0.207$ V vs. SHE (3)

$C + H_2O \rightarrow CO + 2H^+ + 2e^-$, $E^0 = 0.518$ V vs. SHE (4)

Recently novel Ti/Ta_2O_5-SnO_2 electrodes were found potentially active towards electrocatalytic oxidation of organic compounds and particularly methylene blue (MB) dye [22]. However, the best process conditions for electrode preparation and electrocatalytic oxidation of MB still have to be determined. In this paper, we report for the first time on the optimization of the annealing temperature of Ti/Ta_2O_5-SnO_2 electrodes and determine the best media conditions for electrolysis processes in terms of energy and mineralization efficiency.

2 Experimental

2.1 Electrode preparation

Ti/Ta_2O_5-SnO_2 electrodes with the nominal composition of Ta(x) - Sn (100 - x) where x = 7.5 at.% were prepared by a thermal decomposition and drop casting technique of the precursor solution onto a titanium substrate [23]. The detailed preparation method is described elsewhere [22]. The total concentration of metals ions was equal to 0.04 M. The total number of active Ta_2O_5-SnO_2 layers forming the ultrathin film deposited on the titanium substrate was eight. Three different annealing temperatures of 450, 550 and 650 ^{0}C were used for the electrode preparation. After 10 h final air-annealing, without additional air circulation in muffle furnace, the electrodes were cooled down and washed for 10 min in an ultrasonic bath and finally dried at 105 ^{0}C. Electrodes were weighed after etching and at the final stage of preparation. Ta_2O_5-SnO_2 material deposition was equal to 1.1 mg cm^{-2} $\pm$ 3%.

All chemicals used for electrodes and working solution preparation were of analytical grade and used without further purification. Tantalum (V) chloride (99.99% trace metal basis, Sigma-Aldrich), tin (II) chloride dehydrate (≥99.99% trace metals basis, Sigma-Aldrich) and absolute ethanol (Baker Analyzed' VLSI grade, J.T. Baker) were

used for the precursor solution preparation. Titanium substrate pretreatment was conducted in 10 wt.% NaOH (≥98% anhydrous, Sigma-Aldrich) and 18 wt. % boiled hydrochloric acid (pro analysis, Fluka).

2.2 Physicochemical and electrochemical characterization of the electrodes

All electrodes were physically and electrochemically characterized. Microstructure of the produced materials was examined by means of scanning electron microscope (SEM) (Hitachi S-4800, Japan) with an attachment for chemical analysis of specimen in microareas with energy dispersive x-ray spectroscopy (Ametek, S4800, USA). X-ray diffraction (XRD) measurements at small incident angle (GID) were performed using the Empyrean (Panalytical) diffractometer with Cu anode and the focusing mirror. The range of measurement was from 20° to 80° of the angle 2h, with constant omega angle = 1. The measurement step was 0.02°, with measurement time of 2.4 s per step.

The electrochemical characterization of the electrodes was conducted with an Autolab PGSTAT12 Galvanostat/Potentiostat using cyclic voltammetry (CV) measurements in a conventional three electrode cell (200) ml. The potentiostat was computer-controlled by GPES EcoChimie software. The prepared Ti/Ta_2O_5-SnO_2 electrodes, with a surface area of 2.2 cm^2 controlled with Teflon ribbon, were used as working electrodes. Gold disc electrode of 2 mm diameter (Metrohm-Autolab) was used as a working electrode for comparison experiment. A coiled platinum wire served as a counter electrode and saturated calomel electrode (SCE) was used as a reference electrode. All CV measurements were performed versus this reference electrode between 0.15 and 2 V potential limits at a scan rate of 50 mV s^{-1}. Electrode conditioning, at potentials of 0.2 V for 15 s and 1.2 V for 5 s, was applied before each measurement as a pretreatment step. CV measurements were conducted in supporting electrolyte solution of 0.1 M Na_2SO_4 (anhydrous ACS reagent, Sigma-Aldrich), aqueous solution of 0.1 M Na_2SO_4 and 0.1 mM MB (Certistain, Merck) at room temperature in acidic (pH = 2), basic (pH = 12) and neutral (pH = 6.5) media. pH was adjusted by H_2SO_4 and NaOH. An aqueous solution of 0.5 mM potassium hexacyanoferrate (II) trihydrate (99% trace metal basis, Riedel-de-Haën) and 0.1 M Na_2SO_4 was used for CV measurements to estimate the active surface. The supporting electrolyte solution and aqueous solution of Na_2SO_4 and MB are hereafter referred to as the blank and working solution respectively. Ultrapure water (18.2 MΩ cm) was used for the solution preparation and deoxygenated by bubbling nitrogen before every CV measurement. Hielscher UP-50H ultrasonic probe (Sonotrode

MS3, 50 W maximum output power) with 80% amplitude was used for conducting CV measurements in the ultrasonic field.

2.3 Electrolysis and degradation efficiency control

Electrochemical oxidation experiments were carried out in a jacketed reactor placed on a magnetic stirrer. The stirring rate was 1000 rpm. A constant temperature of 25 ± 2 ^{0}C was maintained by water circulation through a jacketed cooler. 30 ml samples of working solution were used for degradation experiments. The Ti/Ta_2O_5-SnO_2 electrodes with a surface area of 2.2 cm^2 were used as anodes and Ti plate of the same surface area served as the cathode. The distance between electrodes was 1 cm. Electrolyses at a constant current of 20 mA (current density of 9 mA cm^{-2}) were carried out using a GW Instek PSM-6003 power supply.

The decolourisation of MB was monitored by UV-Vis spectrophotometer (Lambda 45, Perkin Elmer) by measuring the absorbance of light by MB at 664 nm in neutral and acidic media and at 591 nm in basic media. Chemical Oxygen Demand (COD) was determined by means of a Hach Lange DRB 200 system. The non-purgeable organic carbon (NPOC) content was measured with a TOC analyzer (TOC-Vcpn, Shimadzu, Japan).

The energy consumption (EC) per volume of treated working solution (kWh m^{-3}) and current efficiency (CE, %) of electrolysis processes in different media were calculated according to the following equations [24]:

$$EC\ (kWh\ m^{-3}) = IVt/V_s \quad (1)$$

$$CE\ (\%) = ((\Delta COD)FV_s/8It) \times 100 \quad (2)$$

where I is the average applied current (A), V is the average cell voltage (V), t is the electrolysis time (h in the case of EC) or time of the COD decay (s in the case of CE), V_s is the solution volume (dm^3), ΔCOD is the COD reduction (g dm^{-3}) at time t, F is the Faraday constant (96487 C mol^{-1}) and the constant 8 is the oxygen equivalent mass (q $equiv^{-1}$).

3 Results and Discussion

3.1 XRD analyses and SEM (and EDX)

129 To identify the crystal structure of the prepared electrodes XRD analysis was conducted. Fig. 1 shows XRD patterns
130 of the Ti/Ta_2O_5-SnO_2 electrodes annealed at 450, 550 and 650 ^{0}C. XRD pattern of the electrode annealed at 450 and
131 550 ^{0}C contained intense peaks of hexagonal Ti substrate appearing at 2θ = 35.097, 38.269, 40.141, 52.898, 62.965,
132 70.444, 76.134 and 77.348^0 associated to the (1 0 0), (0 0 2), (1 0 1), (1 0 2), (1 1 0), (1 0 3), (1 1 2) and (2 0 1)
133 crystal orientations of titanium, while XRD patterns of the electrode annealed at 650 ^{0}C showed the only clear peak
134 of hexagonal titanium at 2θ = 40.141^0. This could be explained by high crystallinity of Ta_2O_5 - SnO_2 films formed
135 at 650 ^{0}C. Tantalum was represented by orthorhombic β-Ta_2O_5 with peaks corresponding to the (0 0 1), (1 1 0), (2 0
136 0), (1 1 1), (2 0 1), (0 0 2), (3 1 0), (2 0 2), (3 1 2) and (4 0 2) planes and hexagonal δ-Ta_2O_5 with peaks
137 corresponding to (0 0 3), (2 0 0), (2 0 3), (0 0 6) and (2 2 0). Tetragonal cassiterite SnO_2 was evidenced through the
138 presence of (1 1 0), (1 0 1), (1 1 1), (2 1 1), (3 1 0), (3 0 1), (2 0 2), (3 2 1), (4 0 0) and (3 3 0) reflections. The
139 presence of tetragonal rutile TiO_2 in the Ti/Ta_2O_5-SnO_2 electrodes structure is explained by the oxygen solubility in
140 the metal lattice of the titanium substrate [25]. The main peaks of TiO_2 were corresponding to the (1 0 1), (2 0 0), (1
141 1 1), (2 1 0), (2 1 1), (2 2 0), (0 0 2), (3 1 0), (3 0 1) and (1 1 2) atomic planes. The low intensity of TiO_2, SnO_2 and
142 Ta_2O_5 peaks in the XRD pattern of the electrode annealed at 450 ^{0}C can be attributed to a low crystallinity of the
143 formed oxides and as a result to a low performance of this electrode towards MB oxidation (see below).

144 Fig. 2 shows typical SEM images and EDX element mapping of the Ti/Ta_2O_5-SnO_2 electrodes annealed at 450, 550
145 and 650 ^{0}C. In general, the SEMs show that the surfaces are very similar in appearance although the electrode
146 prepared at 550 °C does have more cavities and pin holes present which tends to suggest a potentially larger active
147 surface area for electrolysis. The surface roughness and porosity can influence diffusion to the electrode surface and
148 this is investigated in section 3.2. From the EDX mapping the Ta distribution (Fig. 2d – f) over Ti substrate is rather
149 scattered with the resulting Ta_2O_5 particles size varying from a few nanometers (dots on the mapping images) to a
150 few micrometers forming agglomerates (bright blue spots). Sn distribution over Ti substrate (Fig. 2g – i) is more or
151 less homogeneous with a greater accumulation on the electrode annealed at 550 ^{0}C and the smaller content on the
152 electrodes annealed at 450 ^{0}C and 650 ^{0}C.

153 *3.2 Cyclic voltammetry*

154 *3.2.1 Characterization of electrodes*

To estimate the relative electrode surface area after annealing, cyclic voltammograms were recorded from an electrolyte containing a simple redox couple, from electrodes prepared at the three chosen annealing temperatures. Figure 3 shows typical cyclic voltammograms recorded for a Ti/Ta_2O_5-SnO_2 electrode annealed at 550 °C from an aqueous solution of 0.5 mM $K_4Fe(CN)_6$ and 0.1 M Na_2SO_4 using a range of potential scan rates. The couple has the characteristics of a quasi-reversible electron transfer on this electrode surface; well-formed oxidation and coupled reduction peaks are observed around 0.25 V and 0.15 V respectively. The peak separations are greater than 60 mV expected for a reversible process (98 mV – 129 mV with the scan rates shown). However, this observation may simply be due to the high intrinsic resistance of this type of electrode material [26]. The value of the diffusion coefficient estimated from the slope of the linear Ip anodic against the square root of the sweep rate plot is $9.2 \cdot 10^{-6}$ $cm^2 s^{-1}$ which is in good agreement with literature reported values [27-30].

Peak currents were recorded from cyclic voltammograms run at slow scan rates. Table 1 shows the peak current densities and peak separations recorded at a sweep rate of 5 mV s^{-1}, for the oxidation of 0.5 mM $K_4Fe(CN)_6$ at three electrode annealing temperatures and for comparison an entry for a gold disc electrode is also included.

Table 1. Peak currents for the oxidation of 0.5 mM $K_4Fe(CN)_6$ in 0.1 M Na_2SO_4 for Ti/Ta_2O_5-SnO_2 electrodes and a Au electrode recorded at a scan rate of 5 mV s^{-1}

Electrode	Annealing temperature, ^0C	Peak Current Density, $\mu A\ cm^{-2}$
Ti/Ta_2O_5-SnO_2	450	41.2
	550	35.4
	650	32.8
Au disc electrode	-	22.1

In general, the peak current densities observed at the Ti/Ta_2O_5-SnO_2 electrodes are of the same order of magnitude with the lowest value recorded for the highest firing temperature. However, the recorded currents are all higher than that recorded from the smooth gold electrode. This observation suggests that Ti/Ta_2O_5-SnO_2 electrodes prepared using the thermal decomposition technique described in [22] and imaged in Figure 2, lead to rough electrode

surfaces with approximately twice the active working area available. It is unclear why the peak currents are reduced at the higher firing temperature of 650 ^{0}C. Other workers have observed similar effects with different oxide electrodes and have suggested that the formation of a poorly conducting oxide layer between the Ta_2O_5-SnO_2 coating and the metal substrate interferes with the electron transfer process [31]. It was found that electrical conductivity of $Sn_{0.97}Ta_{0.03}O_2$ thin films grown on TiO_2 substrates and annealed at 500 – 600 ^{0}C is approximately 1100 S m^{-1} [32]. Trasatti suggests that lower crystallinity may be important. However from the XRD data, see above, a reduced degree of crystallinity was only recorded at 450 ^{0}C and the electron transfer for the ferricyanide redox couple proceeds rapidly at this surface.

3.2.2 MB Oxidation

Fig. 4a shows the CV results of prepared Ti/Ta_2O_5-SnO_2 electrodes recorded from a working solution of 0.1 mM MB and 0.1 M Na_2SO_4. All voltammograms, with the exception of electrode annealed at 450 ^{0}C contained an anodic current peak with a maximum at potential of 1.1 V absent on CVs in the blank solution and attributed to oxidation of MB [22]. Anodic current of 60 μA cm^{-2} at potential of 1.1 V is 3 and 8 times higher for the electrode annealed at 550 ^{0}C than for electrodes annealed at 650 ^{0}C and 450 ^{0}C respectively. The higher capacitance current observed from the electrode annealed at 550 ^{0}C also confirms a greater microroughness. Therefore, at an annealing temperature of 550 ^{0}C the tantalum/tin oxide coating shows some promise as a non-precious metal electrode for the electrocatalytic oxidation of MB. Further investigations at different pHs were carried out to determine the optimum conditions for MB oxidation.

To investigate the electrochemical behavior of prepared Ti/Ta_2O_5-SnO_2 electrodes in different media CVs were run in the working solutions of 0.1 M Na_2SO_4 and MB at pH 2, 6.5 and 12. Figure 4b represents the CV results in 0.1 M Na_2SO_4 and 0.1 mM MB aqueous solution at the pH 2, 6.5 and 12. Voltammograms recorded at pH 6.5 and at pH = 2 showed anodic current peaks of 60 and 30 μA cm^{-2} respectively attributed to the MB oxidation. However, when pH was changed to the value of 12, no anodic current of MB oxidation was observed (Inset Fig. 4b). The absence of MB oxidation peak is explained by a significant shift of the OER onset potential to more negative values from about 1.8 V to 1.4 V and masks the MB oxidation peak. Running an electrolysis process in alkali is therefore more favorable for oxygen formation rather than MB oxidation.

To ensure an efficient electrolysis process the concentration of the electroactive species near the surface of the electrode should be maintained and not depleted. Typically, this is achieved on an industrial scale by efficient agitation of the electrolyte using a number of techniques for example rapid stirring, pumping or using turbulence promoters [33]. Ultrasound can also be used to improve mass transport. The advantages of applying ultrasonic irradiation are twofold: firstly it can increase the movement of electroactive species to the electrode surface and secondly through the process of cavitation hydroxyl radicals can be generated and thereby increase the rate of oxidation of MB.

Figure 5 records the first and sixth cyclic voltammograms from an electrochemical cell without agitation (5a), using a magnetic stirrer (5b) and with a 30 kHz ultrasonic field applied (5c). The cyclic voltammogram without agitation shows the characteristic depletion of the electroactive species and gradually decreases with time whereas stirred and ultrasonically irradiated cells show no change in the current response. The MB is replenished as fast as it is consumed at the electrode surface. Applying ultrasound to any laboratory cell will therefore ensure good electrolyte movement and through cavitation generate radicals which have the potential to accelerate the oxidation of MB.

3.3 Electrolysis (Degradation experiments)

To prove electrocatalytic activity of Ti/Ta_2O_5-SnO_2 electrodes towards MB oxidation and show the effect of different media on MB degradation rates a series of electrolysis experiments was conducted with 0.1 mM MB and 0.1 M Na_2SO_4 solution using magnetic stirring. Preparative electrolysis tests in an ultrasonic field are reported in [34]. According to Fig. 6a 95% and 85% decolourisation efficiency was achieved in two hours of electrolysis at pH of 6.5 and 2 respectively. Degradation rate of MB in basic media was considerably slower and reached only 78% after 2 h of electrochemical oxidation that coincides with the preliminary prediction obtained by CV measurements (Fig. 4b) and was attributed to a low oxygen evolution overvoltage [35-36]. Efficiency of Ti/Ta_2O_5-SnO_2 electrodes in regards of MB oxidation was confirmed by the data on COD and NPOC removal (Fig. 6b, inset Fig. 6a). The fastest COD removal efficiency was obtained at a pH of 6.5 and after 2 h of electrolysis was equal to 85%. It increased slowly to 90% and was stable during 8 h of electrochemical oxidation. Lower COD removal values were achieved after 2h of electrolysis at pH of 2 (70%) and 12 (26%). However, COD removal efficiency increased to 85 – 99% for all media after 8 h of electrolysis. Mineralization data obtained during electrolysis showed that MB was

mostly oxidized to CO_2. Overall NPOC reduction (Inset Fig. 6a) of 71, 74 and 76% was reached after 8 h of electrolysis for the electrodes annealed at 550 ^{0}C at pH of 12, 6.5 and 2 respectively.

Table 2 shows the data on EC required for the complete decolourisation and 80% COD decrease of 0.1 mM MB and 0.1 M Na_2SO_4 solution and CE obtained at 80% COD reduction in different media of working solution. Electrolyses in acidic media was the most energy effective for conducting decolourisation experiments and required 7.7 kWh m^{-3} of energy to achieve 100% colour removal. Basic and original media of working solution needed 24.4 and 21.5 kWh m^{-3} respectively to obtain 100% decolourisation. The EC data are comparable to those required for decolourisation of other organic dyes [37-39]. The original media of working solution was the most energy effective towards COD reduction and basic media was the least effective. The energy required for 80% COD decrease at pH = 6.5 was equal to 9.3 kWh m^{-3} versus 33.9 kWh m^{-3} consumed at pH = 12. The highest CE of 10.1% was observed for the lowest EC of 9.3 kWh m^{-3} required for 80% COD removal at pH = 6.5 that is a typical behavior for many mixed metal oxide electrodes [40-42]. The lowest CE of 1% was obtained for 80% COD decrease in basic conditions which was attributed to oxygen evolution being the favored reaction.

Table 2 EC (kWh m^{-3}) and CE (%) obtained at complete decolourisation and 80% COD reduction of 0.1 mM MB in 0.1 M Na_2SO_4 solution at pH of 6.5, 2 and 12 for the electrodes annealed at 550 ^{0}C and at pH of 6.5 for the electrode annealed at 650 ^{0}C

Electrode annealing temperature and electrolysis media	EC (kWh m^{-3}) at 100% decolourisation	EC (kWh m^{-3}) at 80% COD reduction	CE (%) at 80% COD reduction
550 ^{0}C, pH = 2	7.7	12.9	5.2
550 ^{0}C, pH = 6.5	21.5	9.3	10.1
550 ^{0}C, pH = 12	24.4	33.9	1

4 Conclusion

The annealing temperature of Ti/Ta_2O_5-SnO_2 electrodes and working media for electrocatalytic oxidation of MB was investigated. The electrodes were characterized by XRD, SEM and EDX analysis. Cyclic voltammetry suggested the electrode surface area of Ti/Ta_2O_5-SnO_2 electrodes annealed at 550 °C was high in comparison with

248 an electroplated Pt electrode. An annealing temperature of 550 °C showed the best electrocatalytic activity for
249 oxidation of MB. The original media of the 0.1 M Na_2SO_4 and 0.1 mM MB solutions was found optimal for
250 conducting degradation experiments since it gave high anodic currents of OER and provided decolourisation, COD
251 and TOC removal efficiencies analogous to that in acidic media. Moreover, this media was the most energy effective
252 towards COD decrease providing the lowest value of EC and highest value of CE. Acidic conditions were found
253 energy effective for achieving complete color removal. Decrease of Ti/Ta_2O_5-SnO_2 electrodes efficiency toward MB
254 decolourisation and COD removal during the electrocatalytic oxidation at pH = 12 was observed due to a low OER
255 overvoltage and current leakage for water oxidation. Ultrasonic field showed the improved electrodes performance
256 towards MB oxidation due to enhancement of MB mass transport to the electrode surface which was supported by
257 the data on diffusion controlled process.

258 **Acknowledgments**

259 This work was supported by Maj and Tor Nessling Foundation.

260

261 **References**

262

[1] M. Beck, R. Vallarroel Walker (2013) On water security, sustainability, and the water-food-energy-climate nexus. Front. Environ. Sci. Eng. 7:626 – 639

[2] M. El-Shahawi, A. Hamza, A. Bashammakh, W. Al-Saggaf (2010) An overview on the accumulation, distribution, transformations, toxicity and analytical methods for the monitoring of persistent organic pollutants, Talanta 80:1587 – 1597

[3] U. Pagga, D. Brown (1986) The degradation of dyestuff: Part II behaviour of dyestuff in aerobic biodegradation tests. Chemosphere 15:479 – 491.

[4] C. Comninellis (1994) Electrocatalysis in the electrochemical conversion/combustion of organic pollutants for wastewater treatment. Electrochim. Acta 39:1857 – 1862

[5] J. Fan, G. Zhao, H. Zhao, S. Chai, T. Cao (2013) Fabrication and application of mesoporous Sb-doped SnO_2 electrode with high specific surface in electrochemical degradation of ketoprofen. Electrochim. Acta 94:21 – 29.

[6] R. E. Palma-Goyes, J. Silva-Agredo, I. González, R. A. Torres-Palma (2014)Comparative degradation of indigo carmine by electrochemical oxidation and advanced oxidation processes. Electrochim. Acta 140:427 - 433

[7] A. El-Ghenymy, F. Centellas, J. A. Garrido, R. M. Rodríguez, I. Sirés, P. L. Cabot, E. Brillas (2014) Decolorization and mineralization of Orange G azo dye solutions byanodic oxidation with a boron-doped diamond anode in divided and undivided tank reactors. Electrochim. Acta 130:568 -576

[8] J. M. Aquino, R. Rocha-Filho, L. Ruotolo, N. Bocchi, S. Biaggio (2014) Electrochemical degradation of a real textile wastewater using b-PbO_2 and DSA® anodes. Chem. Eng. J. 251:138 - 145

[9] D. Shao, J. Liang, X. Cui, H. Xu, W. Yan (2014) Electrochemical oxidation of lignin by two typical electrodes: Ti/Sb-SnO_2 and Ti/PbO_2. Chem. Eng. J. 244:288–295

[10] L. Da Silva, D. Franco, L. De Faria, J. Boodts (2004) Surface, kineticsand electrocatalytic properties of Ti/(IrO_2+ Ta_2O_5) electrodes, prepared using controlled cooling rate, for ozone production. Electrochim. Acta 49:3977–3988

[11] L. Xu, Y. Xin, J. Wang (2009) A comparative study on IrO_2-Ta_2O_5coated titanium electrodes prepared with different methods. Electrochim. Acta 54:1820–1825

[12] J. Kong, S. Shi, X. Zhu, J. Ni (2007) Effect of Sb dopant amount on the structure and electrocatalytic capability of Ti/Sb-SnO_2 electrodes in the oxidation of4-chlorophenol. J. Environ. Sci. 19:1380–1386

[13] B. Adams, M. Tian, A. Chen (2009) Design and electrochemical study of SnO_2-based mixed oxide electrodes.

Electrochim. Acta 54:1491–1498

[14] L. Yue, L. Wang, F. Shi, J. Guo, J. Yang, J. Lian, X. Luo (2015) Application of response surface methodology to the decolorization by the electrochemical process using $FePMo_{12}O_{40}$ catalyst. J. Ind. Eng. Chem. 21:971 - 979

[15] M. Zhou, H. Särkkä, M. Sillanpää (2011) A comparative experimental study on methyl orange degradation by electrochemical oxidation on BDD and MMO electrodes. *S*ep. Purif. Technol. 78:290–297

[16] L. García-Cruz, A. Sáez, C. O. Ania, J. Solla-Gullón, T. Thiemann, J. Iniesta, V. Montiel (2014) Electrocatalytic activity of Ni-doped nanoporous carbons in the electrooxidation of propargyl alcohol. Carbon 73:291 – 302

[17] T. Gan, C. Hu, Z. Chen, S. Hu (2011) Novel electrocatalytic system for the oxidation of methyl jasmonate based on layer-by-layer assembling of montmorillonite and phosphotungstic acid nanohybrid on graphite electrode. Electrochim. Acta. 56:4512–4517

[18] Y. Zhao, C. Li, W. Zhao, Q. Du, B. Chi, J. Sun, Z. Chai, X. Wang (2013) Electrocatalytic oxidation of ascorbic acid on a lithium-doped tantalum oxide film coated electrode. Electrochim. Acta 107:52– 58

[19] Y. Wang, Q. Liu, Q. Qi, J. Ding, X. Gao, Y. Zhang, Y. Sun (2013) Electrocatalytic oxidation and detection of N-acetylcysteine based onmagnetite/reduced graphene oxide composite-modified glassy carbon electrode. Electrochim. Acta 111:31– 40

[20] A. Ghonim, B. . El-Anadouli, M. Saleh (2013) Electrocatalytic glucose oxidation on electrochemically oxidized glassy carbon modified with nickel oxide nanoparticles. Electrochim. Acta 114:713– 719

[21] J. Kim, J. Lee, Y. Tak (2009) Relationship between carbon corrosion and positive electrode potential in a proton-exchange membrane fuel cell during start/stop operation. J. Power Sources 192:674–678

[22] M. Shestakova, P. Bonete, R. Gómez, M. Sillanpää, W. Z. Tang (2014) Novel Ti-Ta_2O_5-SnO_2 electrodes for

water electrolysis and electrocatalytic oxidation of organics. Electrochim. Acta 120:302 – 307

[23] C. Comninellis, G. Vercesi (1991) Problems in DSA® coating deposition by thermal decomposition. J. Appl. Electrochem. 21:136–142

[24] C. Martínez-Hutile, E. Brillas (2009) Decontamination of wastewaters containing synthetic organic dyes by electrochemical methods: A general review. Appl. Catal. B-Environ. 87:105 – 145

[25] N. Greenwood, A. Earnshaw (1997) Chemistry of the Elements, 2nd ed., Butterworth-Heinemann, Elsevier, Oxford

[26] M. M. Barsan, E. M. Pinto, M. Florescu, C. M. A. Brett (2009) Development and characterization of a new carbon composite electrode. Anal. Chim. Acta 635:71 – 78

[27] B. K. Gu, Y. A. Ismail, G. M. Spinks, S. I. Kim, I. So, S. J. Kim (2009) A linear actuation of polymeric nanofibrous bundle for artificial muscles. Chem. Mater. 21:511 – 515

[28] E. P. Rivero, F. F. Rivera, M. R. Cruz-Díaz, E. Mayen, I. González (2012) Numerical simulation of mass transport in a filter press type electrochemical reactor FM01-LC: Comparison of predicted and experimental mass transfer coefficient. Chem. Eng. Res. Des. 90:1969-1978

[29] Z. O. Ameur, M. M. Husein (2013) Electrochemical Behavior of Potassium Ferricyanide in Aqueous and (w/o) Microemulsion Systems in the Presence of Dispersed Nickel Nanoparticles. Sep. Sci. Technol. 48:681–689

[30] S. Menolasina (2005) Electrochemical studies of $Fe(CN)_{64}$-/$Fe(CN)_{63}$- on gold ultramicroelectrodes varying the concentrations of KF as supporting electrolyte. Rev. Téc. Ing. Univ. Zulia 28:159 – 168

[31] S. Trasatti (1987) Oxide/aqueous solution interfaces, interplay of surface chemistry and electrocatalysis. Mater. Chem. Phys. 16:157 – 174

[32] H. Toyosaki, M. Kawasaki, Y. Tokura (2008) Electrical properties of Ta-doped SnO_2 thin films epitaxially grown on TiO_2 substrate. Appl. Phys. Lett. 93:132109-1-132109-3.

[33] D. Pletcher, F. Walsh (1990) Industrial Electrochemistry, Springer Science & Business Media

[34] M. Shestakova, M. Vinatoru, T. J. Mason, M. Sillanpää (2015) Sonoelectrocatalytic decomposition of methylene blue using Ti/Ta_2O_5-SnO_2 electrodes. Ultrason. Sonochem. 23:135 – 141

[35] R. Kötz, S. Stucki, B. Carcer (1991) Electrochemical waste water treatment using high overvoltage anodes. Part I: Physiscal and electrochemical properties of SnO_2 anodes. J. Appl. Electrochem. 21:14 – 20.

[36] S. Stucki, R. Kötz, B. Carcer, W. Suter (1991) Electrochemical waste water treatment using high overvoltage anodes. Part II: Anode performance and applications. J. Appl. Electrochem. 21:99 - 104

[37] L. Andrade, L. Ruotolo, R. Rocha-Filho, N. Bocchi, S. Biaggio, J. Iniesta, V. García-Garcia, V. Montiel (2007) On the performance of Fe and Fe,F doped Ti–Pt/PbO_2 electrodes in the electrooxidation of the Blue Reactive 19 dye in simulated textile wastewater. Chemosphere 66:2035-2043

[38] C. Cameselle, M. Pazos, M. Sanromán (2005) Selection of an electrolyte to enhance the electrochemical decolourisation of indigo. Optimisation and scale-up. Chemosphere 60:1080 – 1086

[39] V. López-Grimau, M. Gutiérrez (2006) Decolourisation of simulated reactive dyebath effluents by electrochemical oxidation assisted by UV light. Chemosphere 62:106 – 112

[40] L. Andrade, R. Rocha-Filho, N. Bocchi, S. Biaggio, J. Iniesta, V. García-Garcia, V. Montiel (2008) Degradation of phenol using Co- and Co, F-doped PbO_2 anodes in electrochemical filter-press cells. J. Hazard. Mater. 153: 252 – 260

[41] D. Rajkumar, J. Kim, K. Palanivelu (2005) Indirect electrochemical oxidation of phenol in the presence of chloride for wastewater treatment. Chem. Eng. Technol. 28:98 – 105

[42] Y. Yavuz, A. Koparal (2006) Electrochemical oxidation of phenol in a parallel plate reactor using ruthenium mixed metal oxide electrode. J. Hazard. Mater. 136:296 – 302

263

264 **Figure captures**

265 **Fig. 1** X-Ray diffractograms for Ti/Ta_2O_5-SnO_2 electrodes annealed at 450, 550 and 650 ^{0}C

266 **Fig. 2** SEM images of Ti/Ta_2O_5-SnO_2 electrodes with element-mapping: (d – f) Ta mapping, (g – i) Sn mapping and
267 for the electrodes annealed at (a) 550, (b) 650 and (c) 450 ^{0}C respectively

268 **Fig. 3** CVs Ti/Ta_2O_5-SnO_2 electrode annealed at 550 ^{0}C in 0.5 mM $K_4Fe(CN)_6 \cdot 3H_2O$ and 0.1 M Na_2SO_4 at different
269 scan rates ν

270 **Fig. 4** CV of Ti/Ta_2O_5-SnO_2 electrodes prepared at different temperatures (Fig. 4a) and run in different media (Fig.
271 4b) in working solution of 0.1 mM MB and 0.1 M Na_2SO_4 (Fig 4b) adjusted to of pH = 2 and pH = 12 (Inset Fig.
272 4b) with H_2SO_4 or NaOH respectively for Ti/Ta_2O_5-SnO_2 electrode annealed at 550 ^{0}C. ν = 50 mV s^{-1}

273 **Fig. 5** Different CV scans made in the working solution of 0.1 mM MB and 0.1 M Na_2SO_4 in acidic media (pH = 2)
274 without external exposure (Fig. 5a), under the influence of ultrasonic field (Fig. 5b) and with magnetic stirrer (Fig.
275 5c). ν = 50 mV s^{-1}

276 **Fig. 6** Colour (a) and COD (b) removal efficiency after 8h of electrolysis of 0.1 M Na_2SO_4 and 0.1 mM MB
277 working solution. Inset Fig. 6a: NPOC removal efficiency (mineralization)

278

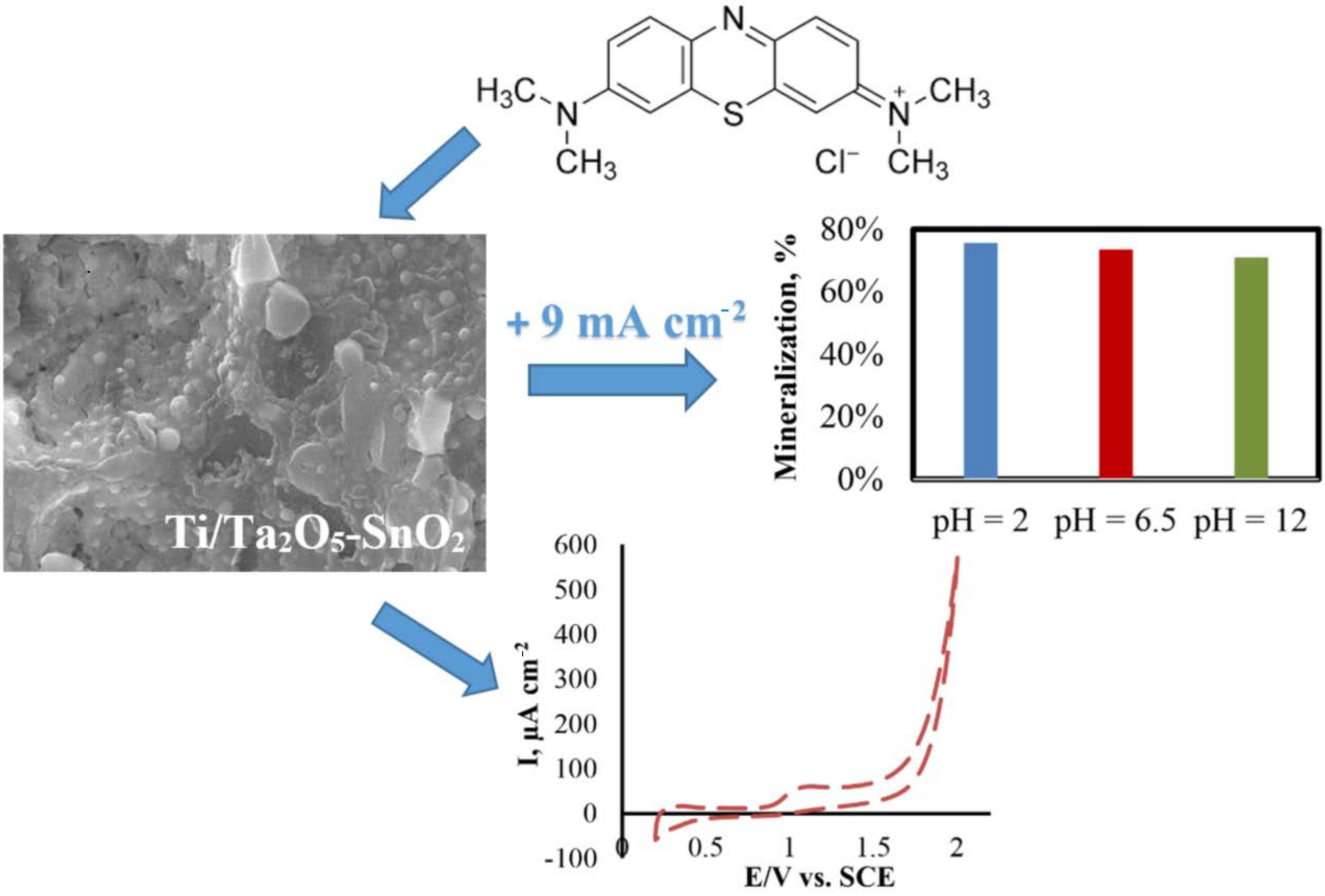
H3C
N
CH3
N
S
N+
CH3
Cl−
CH3
Ti/Ta2O5-SnO2
+ 9 mA cm-2
Mineralization, %
80%
60%
40%
20%
0%
pH = 2
pH = 6.5
pH = 12
I, µA cm-2
600
500
400
300
200
100
0
-100
0
0.5
1
1.5
2
E/V vs. SCE

Table 1. Peak currents for the oxidation of 0.5 mM $K_4Fe(CN)_6$ in 0.1 M Na_2SO_4 for Ti/Ta_2O_5-SnO_2 electrodes and a Au electrode recorded at a scan rate of 5 mV s^{-1}

Electrode	Annealing temperature, ^0C	Peak Current Density, $\mu A\ cm^{-2}$
Ti/Ta_2O_5-SnO_2	450	41.2
	550	35.4
	650	32.8
Au disc electrode	-	22.1

Table 2. EC (kWh m^{-3}) and CE (%) obtained at complete decolourisation and 80% COD reduction of 0.1 mM MB in 0.1 M Na_2SO_4 solution at pH of 6.5, 2 and 12 for the electrodes annealed at 550 ^{0}C and at pH of 6.5 for the electrode annealed at 650 ^{0}C

Electrode annealing temperature and electrolysis media	EC (kWh m^{-3}) at 100% decolourisation	EC (kWh m^{-3}) at 80% COD reduction	CE (%) at 80% COD reduction
550 ^{0}C, pH = 2	7.7	12.9	5.2
550 ^{0}C, pH = 6.5	21.5	9.3	10.1
550 ^{0}C, pH = 12	24.4	33.9	1

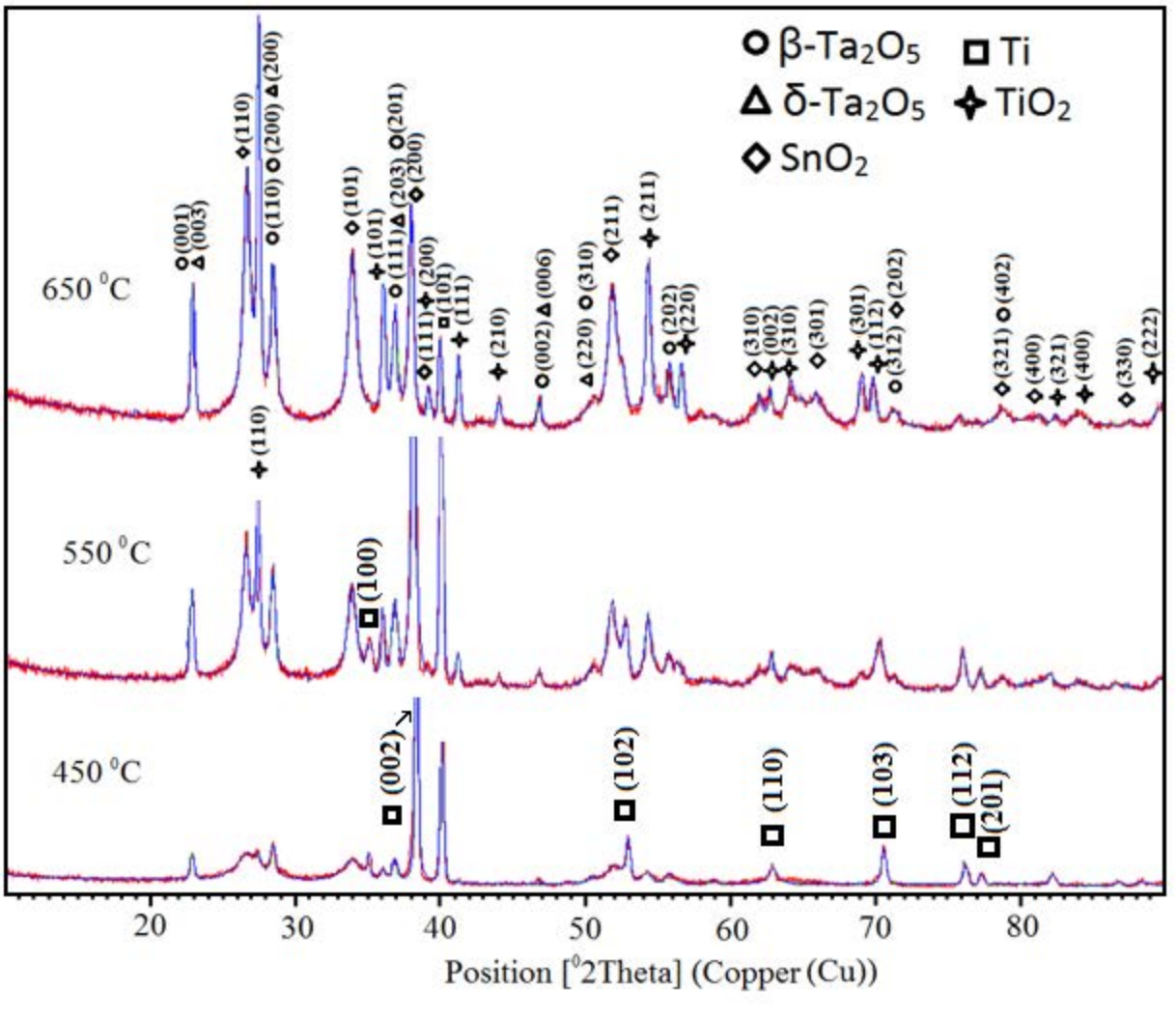
β-Ta2O5
Ti
δ-Ta2O5
TiO2
SnO2
650 °C
550 °C
450 °C
(001)
(003)
(110)
(200)
(110)
(200)
(101)
(101)
(111)
(203)
(201)
(200)
(111)
(200)
(101)
(111)
(210)
(002)
(006)
(220)
(310)
(211)
(211)
(202)
(220)
(310)
(002)
(310)
(301)
(301)
(112)
(312)
(202)
(321)
(402)
(400)
(321)
(400)
(330)
(222)
(110)
(100)
(002)
(102)
(110)
(103)
(112)
(201)
20
30
40
50
60
70
80
Position [°2Theta] (Copper (Cu))

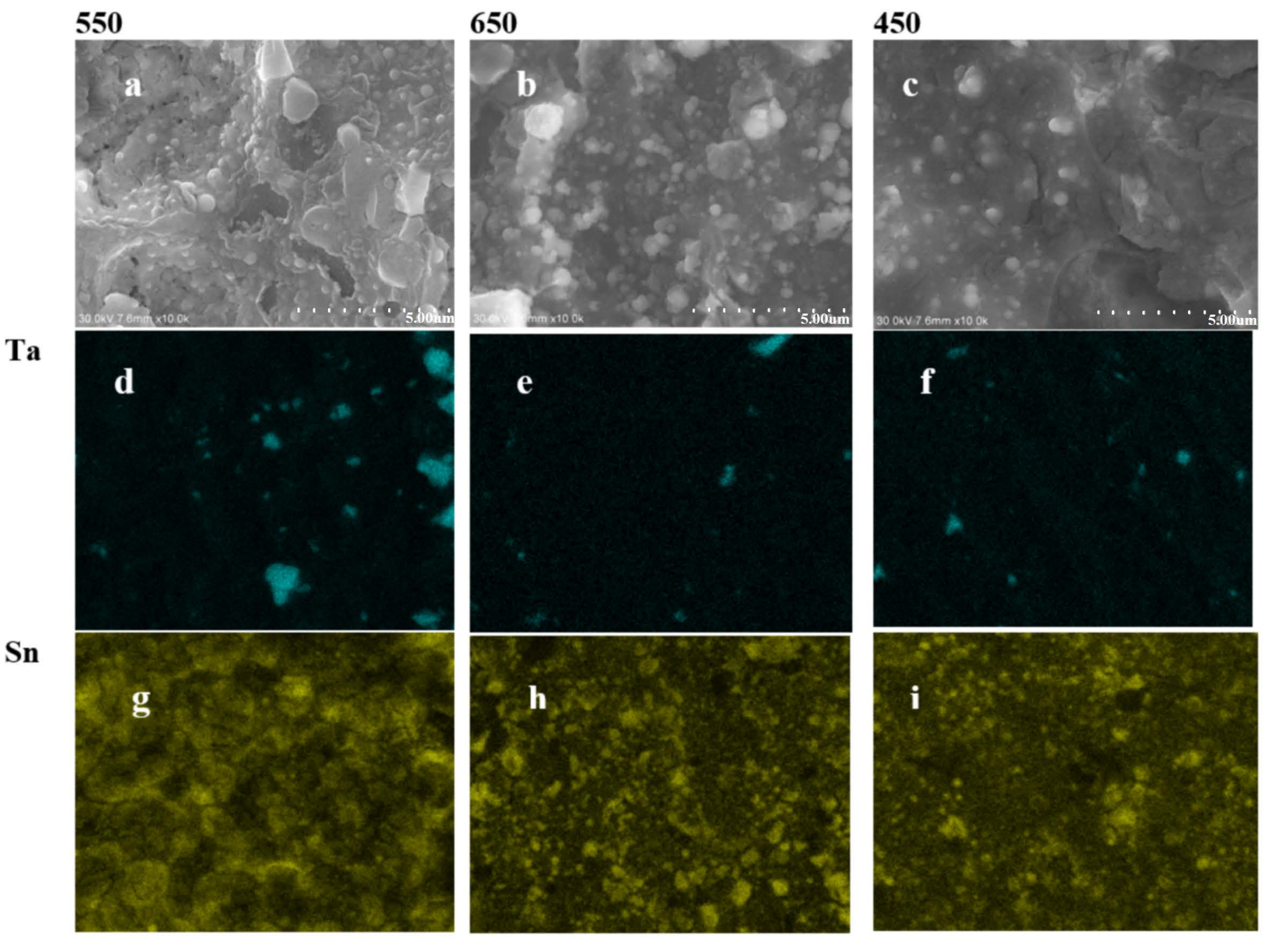
550
650
450
a
b
c
30.0kV 7.6mm x10.0k
5.00um
30.0kV 7.6mm x10.0k
5.00um
30.0kV 7.6mm x10.0k
5.00um
Ta
d
e
f
Sn
g
h
i

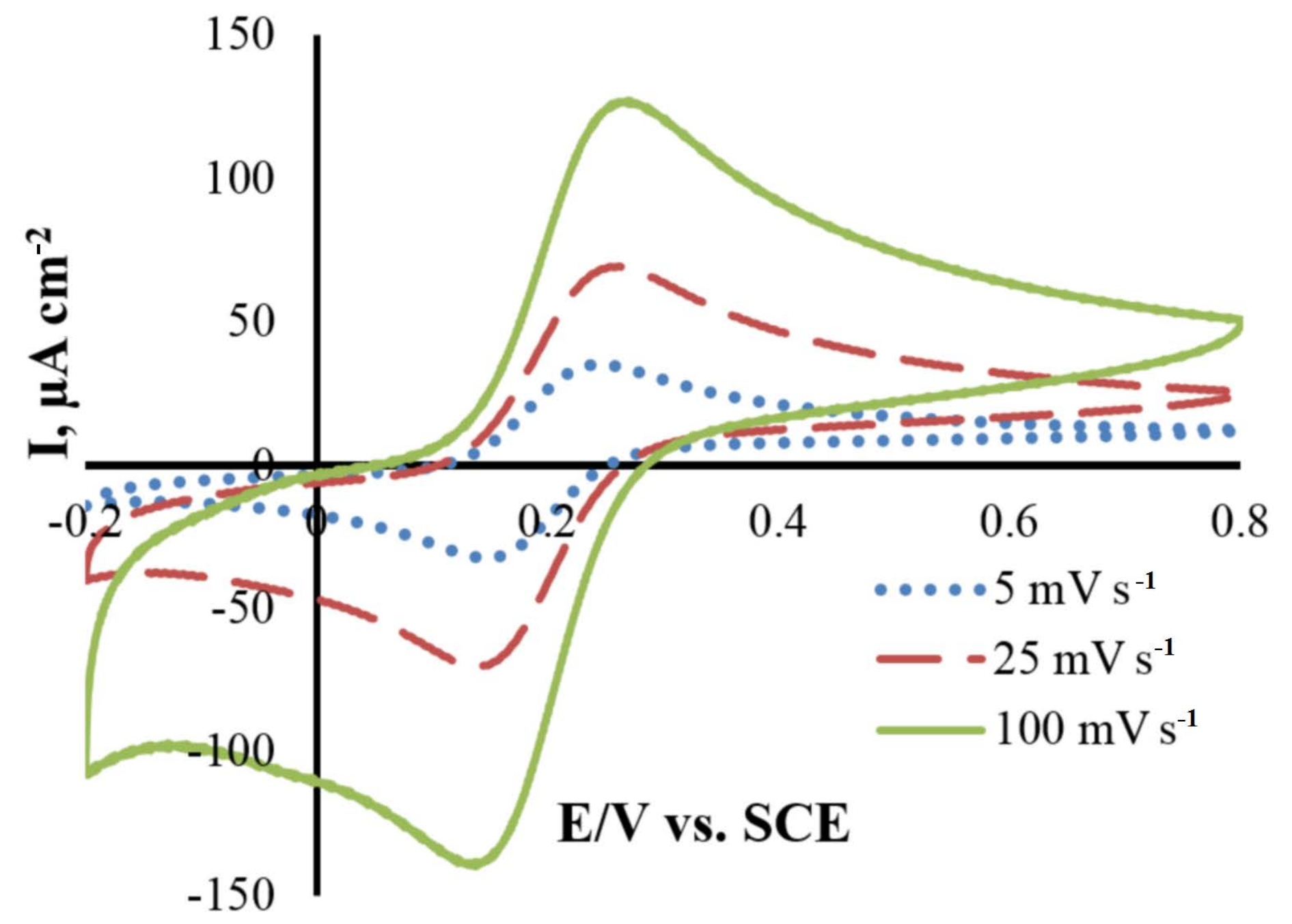
150
100
50
0
-50
-100
-150
-0.2
0
0.2
0.4
0.6
0.8
I, µA cm-2
E/V vs. SCE
5 mV s-1
25 mV s-1
100 mV s-1

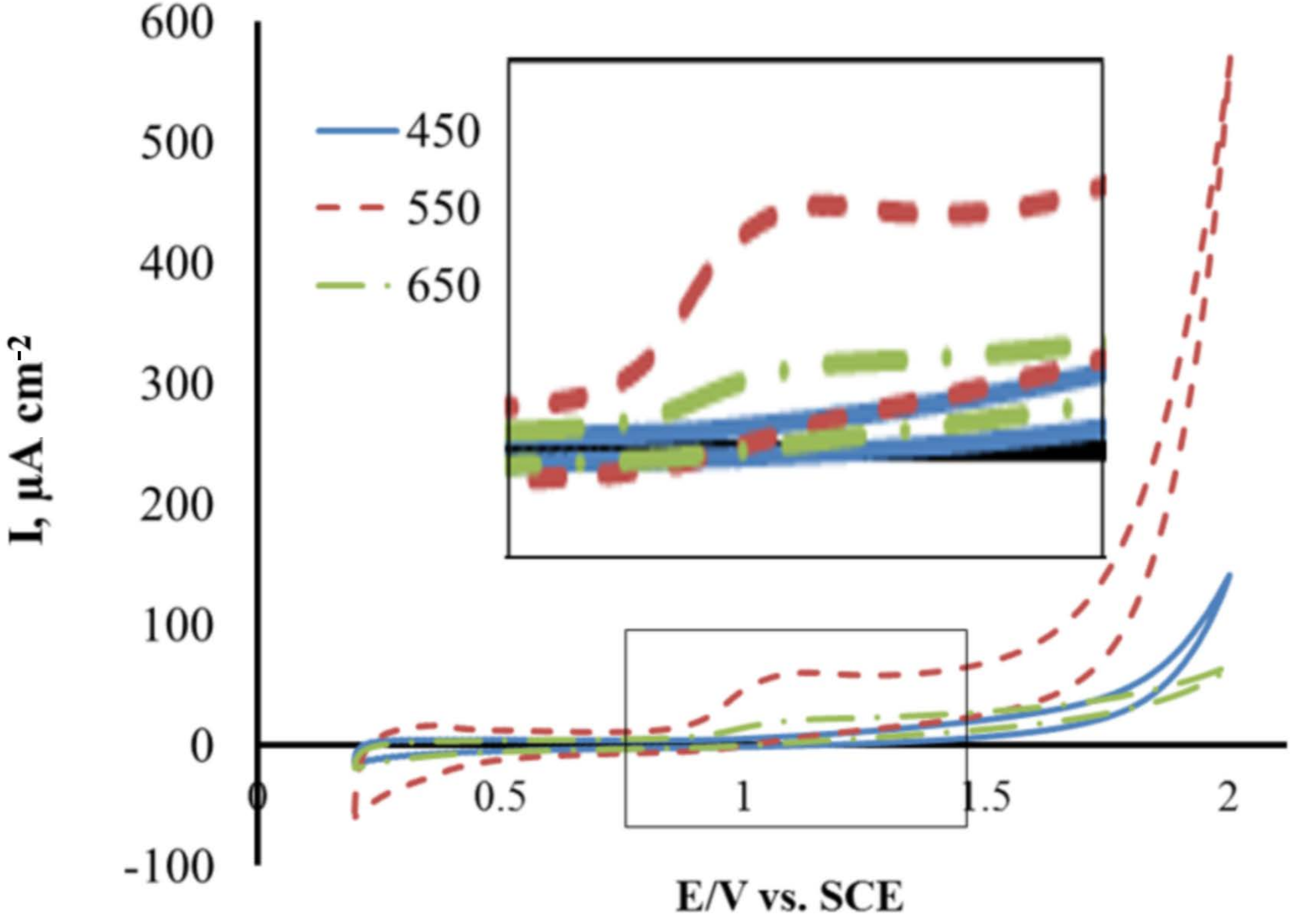
600
500
400
300
200
100
0
-100
0
0.5
1
1.5
2
450
550
650
I, µA cm-2
E/V vs. SCE

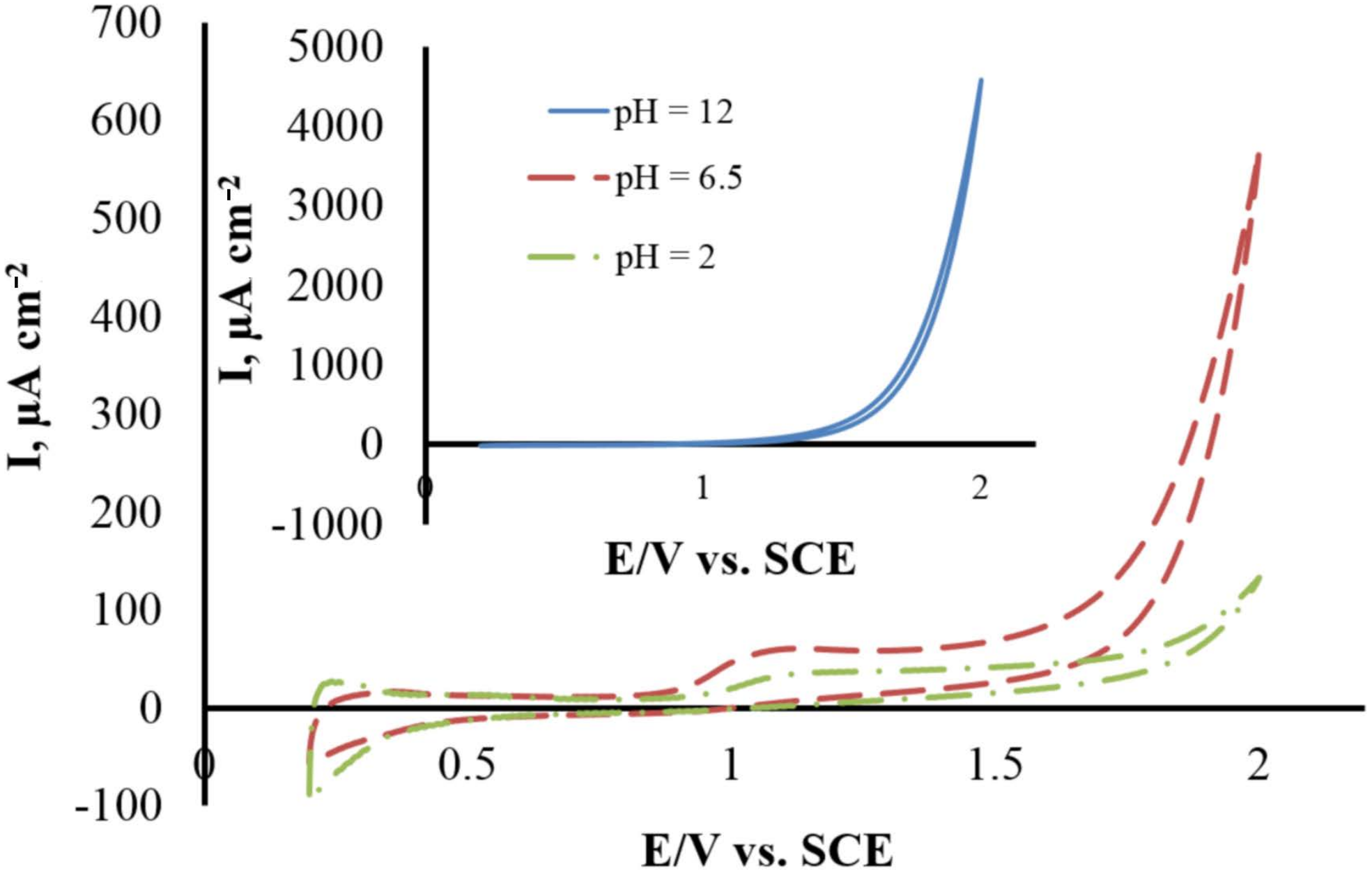
700
600
500
400
300
200
100
0
-100
I, µA cm-2
0
0.5
1
1.5
2
E/V vs. SCE
5000
4000
3000
2000
1000
0
-1000
I, µA cm-2
pH = 12
pH = 6.5
pH = 2
0
1
2
E/V vs. SCE

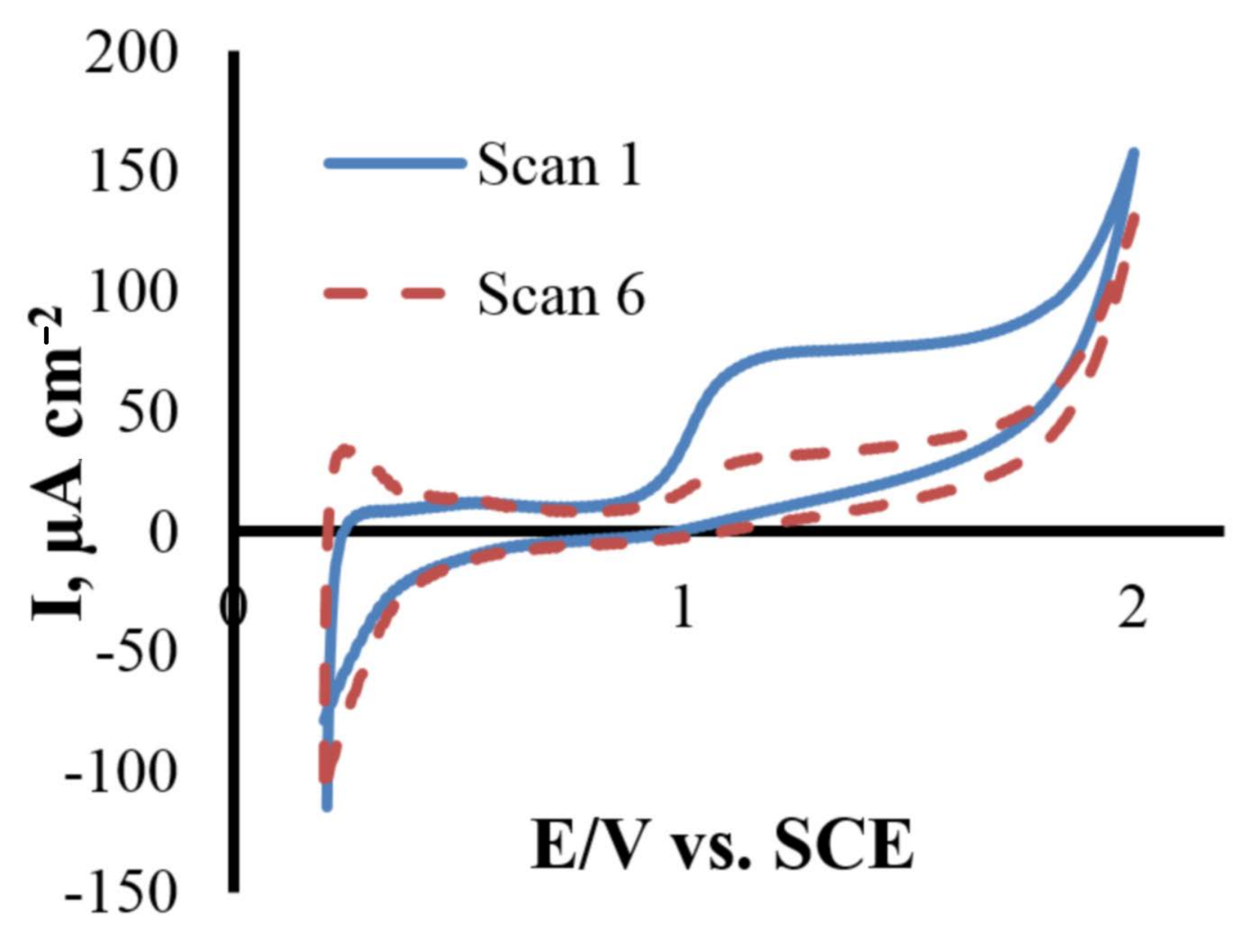
200
150
100
50
0
-50
-100
-150
I, µA cm-2
0
1
2
E/V vs. SCE
Scan 1
Scan 6

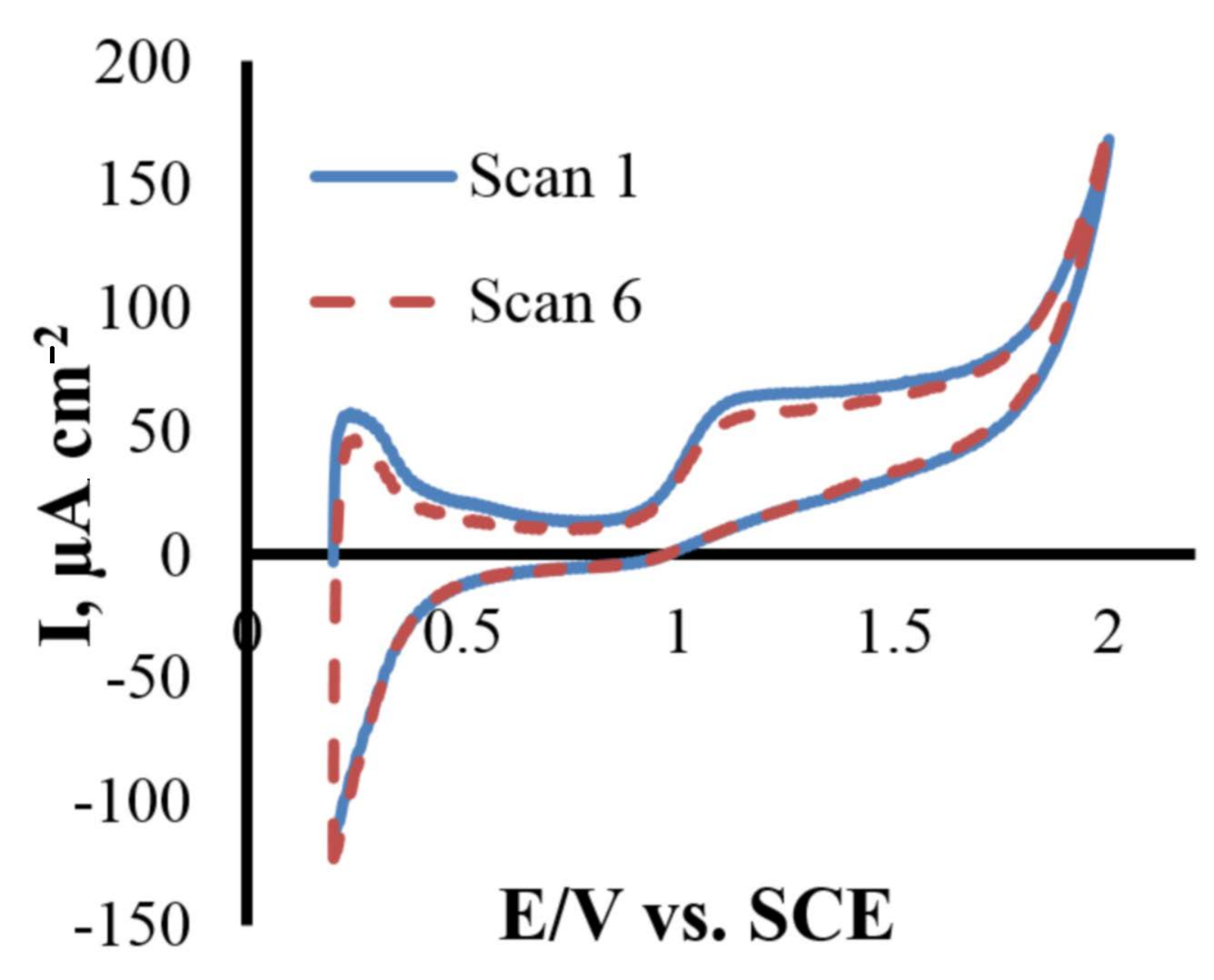
200
150
100
50
0
-50
-100
-150
I, µA cm-2
0
0.5
1
1.5
2
E/V vs. SCE
Scan 1
Scan 6

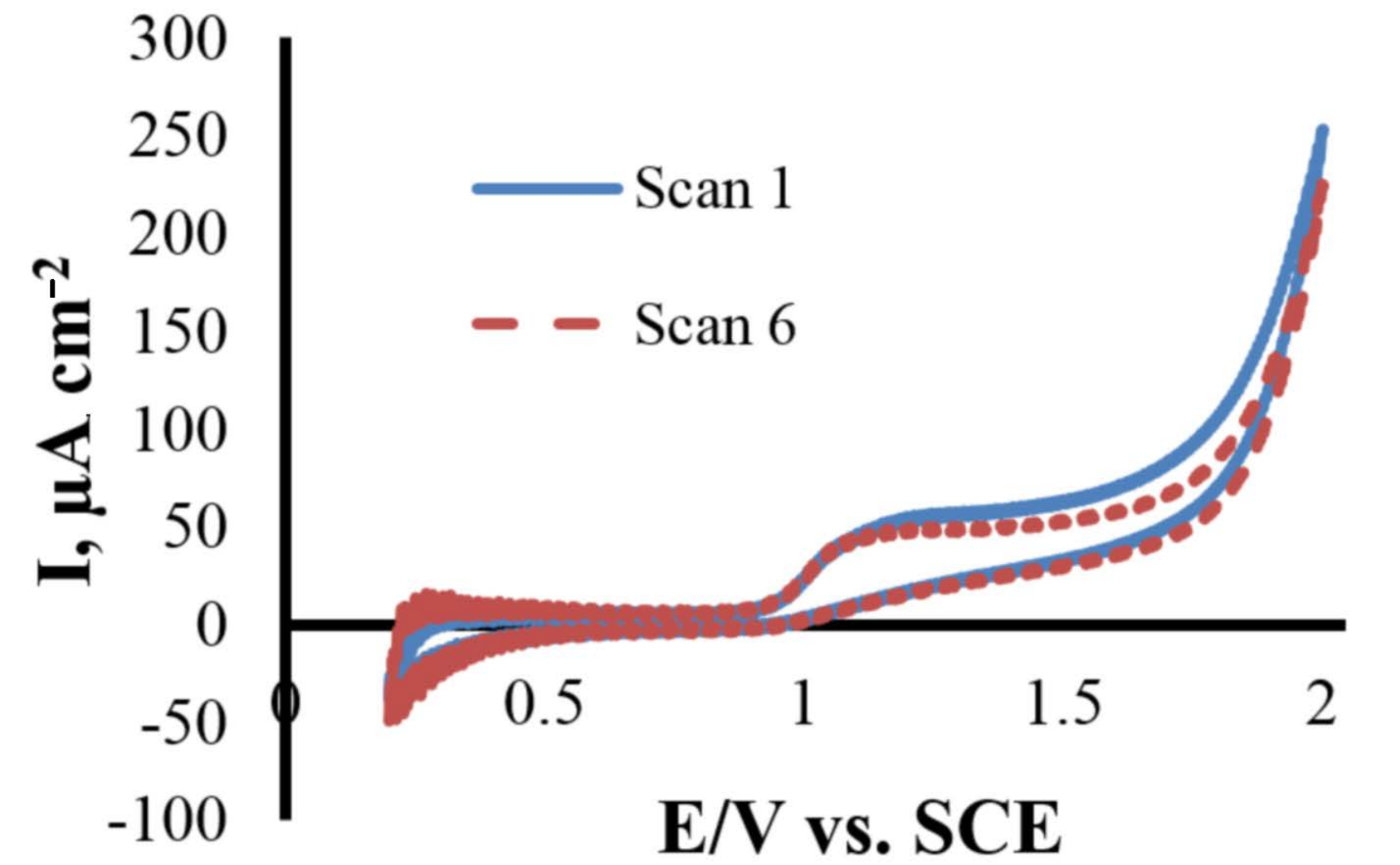
300
250
200
150
100
50
0
-50
-100
I, μA cm-2
Scan 1
Scan 6
0
0.5
1
1.5
2
E/V vs. SCE

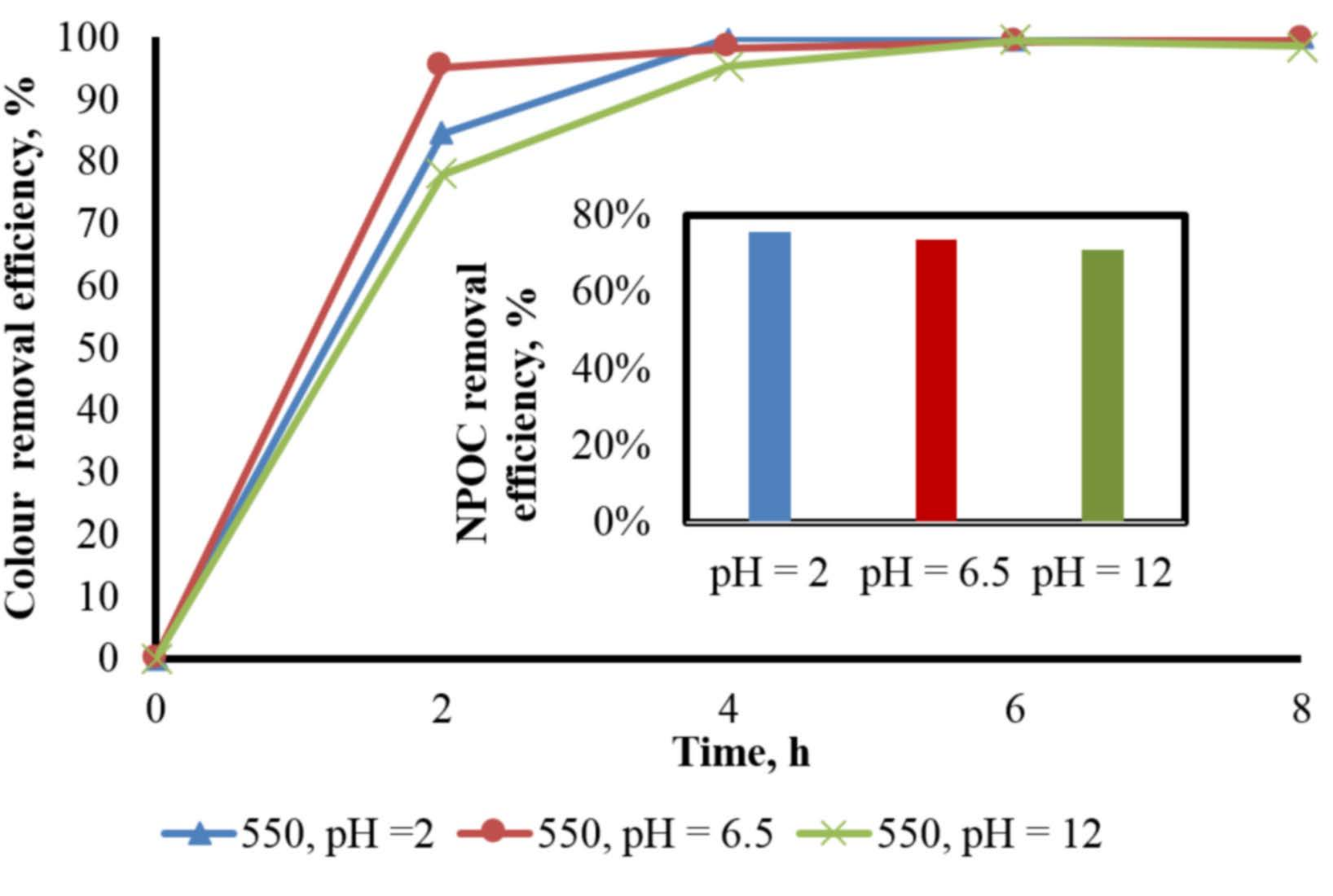
Colour removal efficiency, %
100
90
80
70
60
50
40
30
20
10
0
0
2
4
6
8
Time, h
NPOC removal efficiency, %
80%
60%
40%
20%
0%
pH = 2
pH = 6.5
pH = 12
550, pH =2
550, pH = 6.5
550, pH = 12

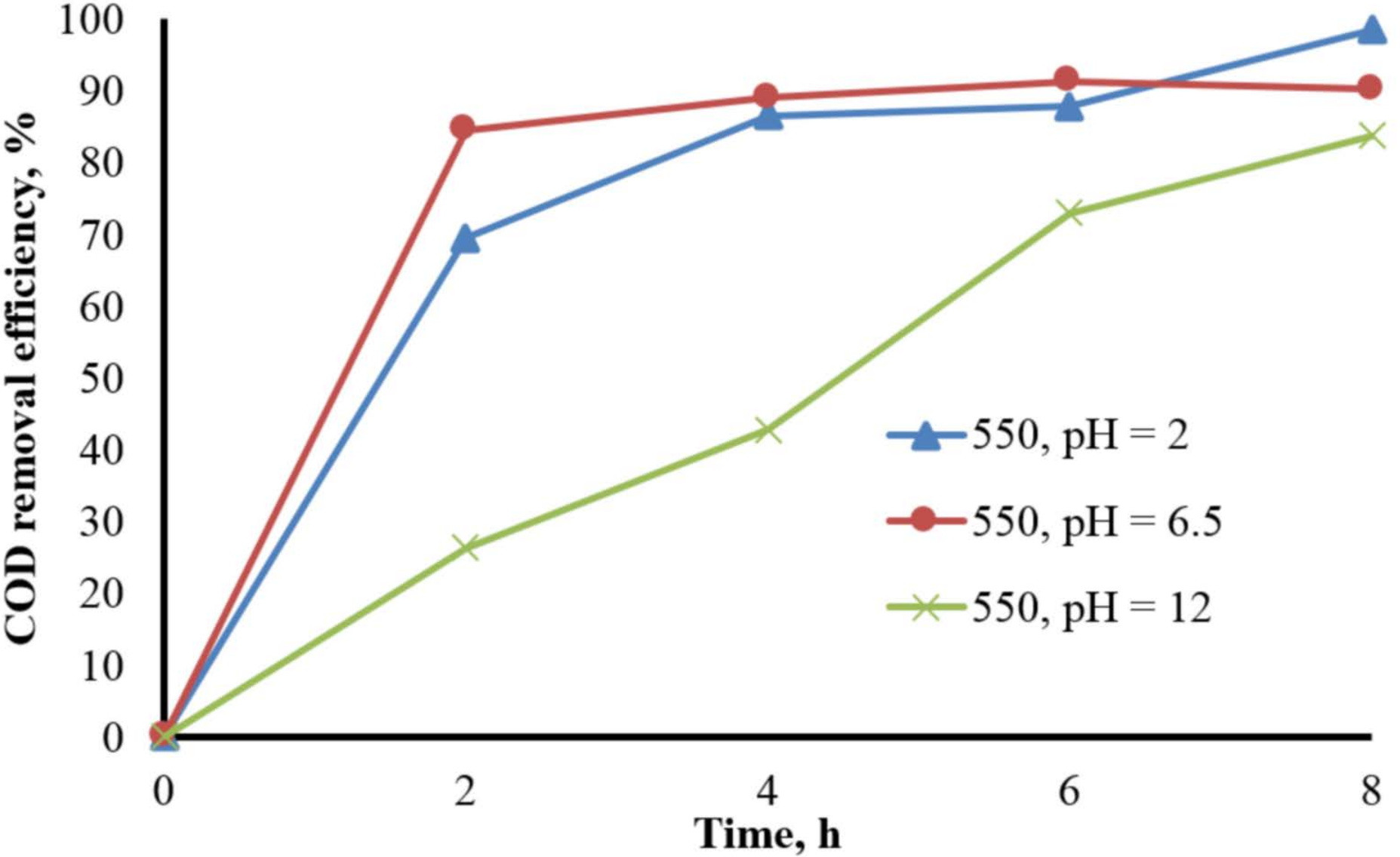
COD removal efficiency, %
100
90
80
70
60
50
40
30
20
10
0
0
2
4
6
8
Time, h
550, pH = 2
550, pH = 6.5
550, pH = 12